Structural and Magnetic Properties of Monomeric and Dimeric Copper(II) Complexes with Phenyl-*N*-[(pyridine-2-yl)methylene]methaneamide

Hong Woo Lee,[†] Nallathambi Sengottuvelan, Hoe-Joo Seo,[†] Jae Soo Choi,[‡] Sung Kwon Kang,[‡] and Young-Inn Kim[*]

Department of Chemistry Education and Center for Plastic Information System, Pusan National University, Pusan 609-735, Korea. [*]E-mail: yikim@pusan.ac.kr
[†]Department of Chemistry, Pusan National University, Pusan 609-735, Korea
[‡]Department of Chemistry, Chungnam National University, Daejeon 305-764, Korea
Received May 9, 2008

The reaction of copper(II) chloride with phenyl-*N*-[(pyridine-2-yl)methylene]methaneamide (ppmma) leads to a new μ-chloro bridged dimeric [Cu(ppmma)Cl$_2$]$_2$ complex, whereas a reaction of copper(II) bromide with ppmma affords a monomeric Cu(ppmma)Br$_2$ complex. Both complexes have been characterized by X-ray crystallography and electronic absorption spectroscopy. The crystal structural analysis of [Cu(ppmma)Cl$_2$]$_2$ shows that the two Cu(II) atoms are bridged by two chloride ligands, forming a dimeric copper(II) complex and the copper ion has a distorted square-pyramidal geometry ($\tau = 0.2$). The dimer units are held through a strong intermolecular π-π interactions between the nearest benzyl rings. On the other hand, Cu(ppmma)Br$_2$ displayed a distorted square planar geometry with two types of strong intermolecular π-π interaction. EPR spectrum of [Cu(ppmma)Cl$_2$]$_2$ in frozen glass at 77 K revealed an equilibrium between the mononuclear and binuclear species. The magnetic susceptibilities data of [Cu(ppmma)Cl$_2$]$_2$ and Cu(ppmma)Br$_2$ follow the Curie-Weiss law. No significant intermolecular magnetic interactions were examined in both complexes, and magnetic exchange interactions are discussed on the basis of the structural features.

Key Words : Monomeric copper(II) complex, Dimeric copper(II) complex, Magneto-structural relationships, π-π Interaction

Introduction

Current research work concerning the structural and magnetic properties of polynuclear transition metal compounds is aimed at understanding the structural and chemical features governing electronic exchange coupling through multi-atom bridging ligands [1-3] and possibilities for magnetic interaction between the two metal ions, leading to the design of molecular magnetic materials.[4] The pyridine-based bridging ligands have been actively utilized as construction units to obtain lots of supramolecular arrays and molecular magnetic materials.[5-7] Furthermore, the weak forces such as hydrogen bonding, van der Waals forces, π-π interactions and dipole-dipole interactions are very common in constructing these types of systems.[8-11] The small changes in structure can have important effects on the magnetic properties of these systems. In order to develop a correlation between the molecular structure and magnetic behavior, we have undertaken a systematic study of several copper complexes of multidentate ligands containing a pyridine ring with a halo-bridged structure.[12,13] As a part of this program, we have focused on the preparation, characterization and magnetism of copper(II) complexes of [Cu(ppmma)Cl$_2$]$_2$ and Cu(ppmma)Br$_2$ together with the X-ray crystal structure determination. In our recent observation,[12] crystal structure determinations of [Cu(dmamhp)X$_2$]$_2$ complexes (where dmamhp = 2-dimethylaminomethyl-3-hydroxy pyridine) have revealed that both chloride and bromide complexes form dimeric structures, but interestingly, in the present situation, chloride is dimeric while analogous bromide is a monomeric complex.

Experimental Section

All reagents and solvents for syntheses and analyses were purchased from the Aldrich Chemical Company and were used as received.

Synthesis of ligand. Pyridine-2-carboxyaldehyde (2.14 g, 20 mmol) was added slowly to benzylamine (2.14 g, 20 mmol) in isopropylalcohol (50 mL) and the mixture was refluxed for 12 h. On cooling, the product was obtained as yellow oil. Yield: 2.9 g (74%) Selected IR data (KBr, cm^{-1}): 3059, 2882 (s, $\nu_{C\text{-}H}$), 1586 (s, $\nu_{C=N}$), 1647, 1436, 617 (s, $\nu_{\text{pyridine ring}}$).

^{1}H NMR (300 MHz, CDCl$_3$, ppm): δ 2.14 (s, 2H), 7.27 (m, H) 7.29 (d, 4 H), 7.34 (s, H), 7.71 (t, 2H), 8.05 (d, H), 8.63 (d, H). The synthetic pathway is shown in Scheme 1.

Synthesis of complex [Cu(ppmma)Cl$_2$]$_2$. An isopropylalcohol solution (20 mL) of CuCl$_2$ (10 mmol) was added dropwise to a ppmma (10 mmol) isopropylalcohol solution (20 mL). The yellow-greenish powder was precipitated immediately. The resulting mixture was stirred for approximately one hour. The resultant yellow-green precipitate was collected by filtration and washed several times with cold methanol. The precipitates were dried over vacuum in an oven at room temperature. The dried yellowish green powders were recrystallized in acetonitrile. The crystals suitable for X-ray analysis were obtained by slow evapo-

1712 *Bull. Korean Chem. Soc.* **2008**, Vol. 29, No. 9

Hong Woo Lee *et al.*

Phenyl-N-[(pyridine-2-yl)methylene}
methaneamide (ppmma)

(ppmma)CuBr$_2$

[(ppmma)CuCl$_2$]$_2$
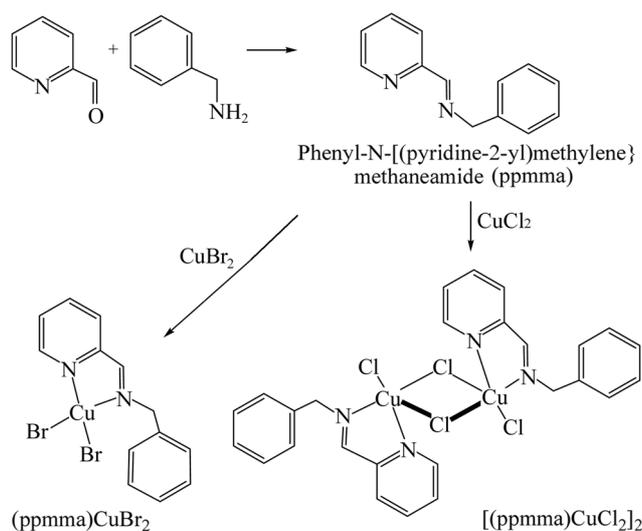
Scheme 1

ration from this solution. Elemental analyses were performed at the Korean Basic Science Institute using Vario-EL III elemental analyzer. Yield: 2.6 g (78%); *Anal.* Calc. for C$_{26}$H$_{24}$Cl$_4$Cu$_2$N$_4$: C, 47.21; H, 3.66; N, 8.47. Found: C, 48.44; H, 4.04; N, 8.36; Selected IR data (KBr, cm^{-1}): 3028, 2921 (s, ν_{C-H}), 1598 (s, $\nu_{C=N}$), 1642, 1449, 608 (s, $\nu_{pyridine\ ring}$).

Synthesis of Cu(ppmma)Br$_2$. This compound was obtained as dark purple crystals in a reaction similar to that of [Cu(ppmma)Cl$_2$]$_2$, except for the use of CuBr$_2$ (0.1 mmol), instead of CuCl$_2$. Yield: 3.2 g (76%); *Anal.* Calc. for C$_{13}$H$_{12}$Br$_2$CuN$_2$: C, 37.21; H, 2.88; N, 6.68. Found: C, 37.95; H, 3.05; N, 6.70; Selected IR data (KBr, cm^{-1}): 3029, 2925 (s, ν_{C-H}), 1599 (s, $\nu_{C=N}$), 1641, 1450, 605 (s, $\nu_{pyridine\ ring}$).

Physical measurements. Electronic absorption spectra were recorded at ambient temperature on a Jasco V-570 UV/vis/NIR spectrophotometer. The X-band EPR spectra of powder materials and frozen glass samples (Toluene/Methanol) at 77 K were recorded on an ESP-300S EPR spectrometer. The field modulation frequency was 100 kHz, and diphenylpicrylhydrazyl (DPPH) was used as a reference. The variable temperature magnetic susceptibilities were measured on a Magnetic Property Measurement System (MPMS7) Quantum Design by SQUID method. The susceptibilities data was corrected for the diamagnetism of the constituent atoms with Pascal's constants and for the temperature-independent paramagnetism of the copper, which was estimated to be 60 × 10^{-6} cgsu/Cu atom.

X-ray single crystal structural analysis. X-ray intensity data was collected at room temperature on a Bruker SMART APEX-II CCD diffractometer using graphite monochromated Mo Kα radiation. Structures were solved by applying the direct method using a SHELXS-97 and refined by a full-matrix least-squares calculation on F^2 using SHELXL-97.[14] All non-hydrogen atoms were refined anisotropically. All hydrogen atoms were placed in ideal positions and were riding on their respective carbon atoms ($B_{iso} = 1.2\ B_{eq}$).

Results and Discussion

Description of structure. Single crystals of [Cu(ppmma)-Cl$_2$]$_2$ and Cu(ppmma)Br$_2$ were recrystallsed from acetonitrile solution and characterized using X-ray crystallography. The X-ray crystal structures of [Cu(ppmma)Cl$_2$]$_2$ and Cu(ppmma)-Br$_2$ are shown in Figure 1. The crystallographic data and structure refinement parameters of the [Cu(ppmma)Cl$_2$]$_2$ and Cu(ppmma)Br$_2$ are summarized in Table 1. The selected bond lengths and bond angles are given in Table 2. It is interesting that [Cu(ppmma)Cl$_2$]$_2$ consists of a dimeric structure whereas Cu(ppmma)Br$_2$ forms a monomeric structure, and both complexes have π-π interactions in the unit cell.

Each copper atom of the dimeric unit of [Cu(ppmma)Cl$_2$]$_2$ is five-coordinated and the geometry around the Cu(II) ion has a regular square based pyramidal environment with atoms N1, N8 of ppmma, Cl2 from the bridged chlorine and terminal Cl1 atoms forming the square plane. The Cl2' occupies the axial position. The structural index τ, $[\beta - \alpha]/60$ with α and β being the two largest angles, is zero for an ideal square pyramid and becomes an unity for an ideal trigonal bipyramid.[15] The calculated τ value of [Cu(ppmma)-Cl$_2$]$_2$ is 0.21 (where $\alpha = 161.06$ and $\beta = 173.40$) indicating that the geometry has nearly a regular square based pyramidal structure. The distance of Cu-Cu is 3.5103(7) Å. The Cu-Cl-Cu bridge is formed by atoms Cu, Cl2, Cl2' and Cu' (symmetry code: (i) −x+1, −y+1, −z); the bridging Cu$_2$Cl$_2$ unit is planar with a crystallographic inversion center. The two unequal central Cu-Cl bond distances in the bridged

a

b
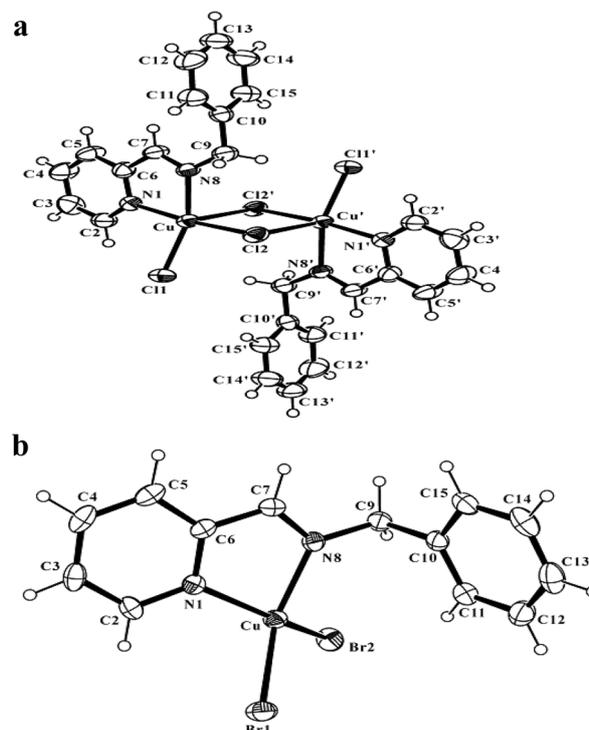
Figure 1. The molecular structures of [Cu(ppmma)Cl$_2$]$_2$ (a) and Cu(ppmma)Br$_2$ (b), showing the atom-numbering schemes [symmetry code: (i) −x+1, −y+1, −z+2.] and 30% probability ellipsoid.

Table 1. Crystal data and details of refinement for [Cu(ppmma)Cl$_2$]$_2$ and Cu(ppmma)Br$_2$

	[Cu(ppmma)Cl$_2$]$_2$	Cu(ppmma)Br$_2$
Empirical formula	C$_{26}$H$_{24}$N$_4$Cl$_4$Cu$_2$	C$_{13}$H$_{12}$N$_2$Br$_2$Cu
Formula weight (amu)	661.37	416.61
Temperature (K)	295(2)	295(2)
Wavelength (Å)	0.71073	0.71073
Crystal system, Space group	Triclinic, *P*-1	Monoclinic, *P*2$_1$/*n*
Unit cell dimensions		
a (Å) & α (°)	8.22230(6) & 77.806(4)	8.2026(5) & 90.00
b (Å) & β (°)	8.8469(7) & 72.323(4)	12.3228(9) & 96.960(3)
c (Å) & γ (°)	10.7596(7) & 66.345(4)	13.7943(9) & 90.00
Volume (Å^3)	679.53(9)	1384.04(16)
Z, Calculated density (Mg/m^3)	2, 1.616	4, 2.014
μ (mm^{-1})	1.981	7.334
F(000)	668	812
Crystal size (mm)	0.15 × 0.16 × 0.17	0.17 × 0.14 × 0.13
θ Range (°)	2.00-27.50	2.98-28.25
Limiting indices	−10 ≤ h ≤ 10; −11 ≤ k ≤ 11; −13 ≤ l ≤ 13	−10 ≤ h ≤ 9; −16 ≤ k ≤ 14; −18 ≤ l ≤ 18
Reflections collected/ unique	12547/3033[R(int) = 0.0282]	10055/3319[R(int) = 0.0577]
T_{max} & T_{min}	0.732 & 0.670	0.320 & 0.380
Refinement method	Full-matrix least-squares on F^2	Full-matrix least-squares on F^2
Data/restraints/parameters	3033 / 0 / 163	3319 / 0 / 163
Goodness-of-fit on F^2	1.063	0.947
Final R indices [$I > 2\sigma(I)$]	$R_1 = 0.0296$, $wR_2 = 0.0704$	$R_1 = 0.0391$, $wR_2 = 0.0662$
R indices (all data)	$R_1 = 0.0425$, $wR_2 = 0.0844$	$R_1 = 0.0879$, $wR_2 = 0.0808$
$\Delta\rho_{max}$ and $\Delta\rho_{min}$ (e Å^{-3})	0.313 and −0.287	0.419 and −0.445

Table 2. Selected bond lengths (Å) and angles (°) of [Cu(ppmma)-Cl$_2$]$_2$ and Cu(ppmma)Br$_2$

[Cu(ppmma)Cl$_2$]$_2$

Bond distances (Å)		Bond angles (°)	
Cu-N1	2.028(2)	N1-Cu-N8	80.03(8)
Cu-N8	2.047(2)	N1-Cu-Cl1	92.56(6)
Cu-Cl1	2.2530(7)	N8-Cu-Cl1	161.06(6)
Cu-Cl2	2.2613(7)	N1-Cu-Cl2	173.40(6)
Cu-Cl2^i	2.6957(8)	N8-Cu-Cl2	93.41(6)
Cu...Cu^i	3.5103(7)	Cl1-Cu-Cl2	93.91(3)
Cl2-Cu^i	2.6957(8)	N1-Cu-Cl2^i	89.17(6)
		N8-Cu-Cl2^i	91.10(6)
		Cl1-Cu-Cl2^i	106.31(3)
		Cl2-Cu-Cl2^i	90.27(2)
		Cu-Cl2^i-Cu^i	89.73(2)

Cu(ppmma)Br$_2$

Bond distances (Å)		Bond angles (°)	
Cu-N1	1.994(3)	N1-Cu-N8	81.34(14)
Cu-N8	2.019(3)	N1-Cu-Br1	96.03(10)
Cu-Br1	2.3526(7)	N8-Cu-Br1	145.06(11)
Cu-Br2	2.3494(7)	N1-Cu-Br2	149.47(10)
		N8-Cu-Br2	98.86(11)

Symmetry transformations used to generate equivalent atoms: (i) −x+1, −y+1, −z+2

Cu$_2$Cl$_2$ unit are 2.2613(7) and 2.6957(8) Å, which are longer than the terminal Cu-Cl1 distance 2.2530(7) Å. The Cu-Cl-Cu angle is 89.73°. These values are normal as observed in other dimeric copper chloride compounds.[16] The study of the crystal packing (Figure 2a) of dimeric [Cu(ppmma)Cl$_2$]$_2$ complex shows that the structure is stabilized by a strong
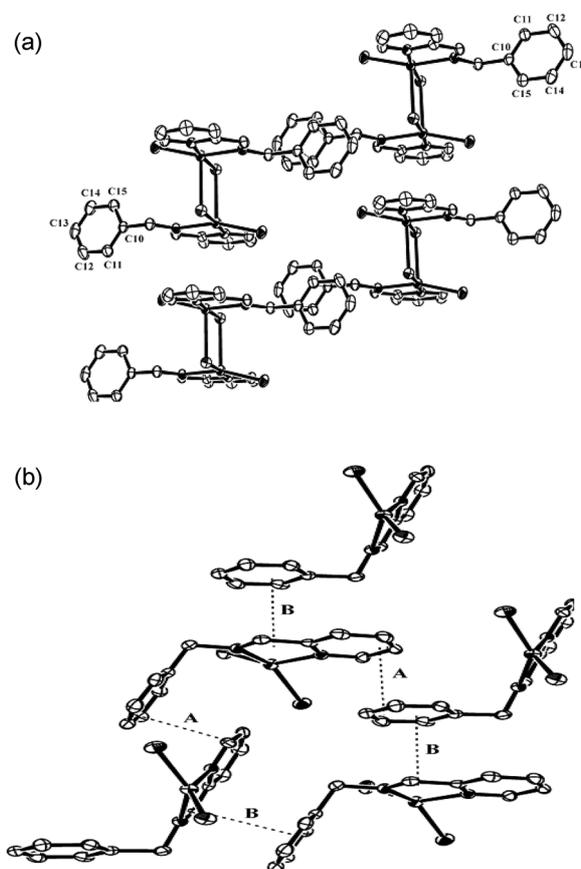
Figure 2. The molecular packing diagram of [Cu(ppmma)Cl$_2$]$_2$ (a) and Cu(ppmma)Br$_2$ (b), π-π interactions are shown with short-dashed lines.

intermolecular π-π interaction between the nearest benzyl rings in the two dimeric $[Cu(ppmma)Cl_2]_2$ complexes. The distance of the nearest benzyl ring is 3.4 Å, which is very similar value to the distance of the π-π interaction in graphite.

In the $Cu(ppmma)Br_2$ complex, the copper is coordinated *via* two N atoms from ppmma and two bromide atoms to complete its tetra-coordination. The angles around Cu are in the range of 81.34-149.47°, suggesting that the geometry around the copper center has a distorted square planar geometry. The dihedral angle between the N1-Cu-N8 and Br1-Cu-Br2 plane is 44.81(11)°, which is smaller than 90° for the perfect tetrahedron. The lack of formation of a dimer may be due to the bulky bromide atom resulting in the formation of a larger dihedral angle than the general square planar structure. A molecular packing diagram for the $Cu(ppmma)Br_2$ complex is shown in Figure 2b. The $Cu(ppmma)Br_2$ are stabilized through two kinds of π-π interaction (A and B type in figure). The distances of A type and B type are 3.28 Å (deviation of C2-C3-C4 plan and C14^i) and 3.40 Å (deviation of C6-C7-N8 and C14^{ii}), respectively. These values are shorter than the distance of the π-π interaction in graphite, which indicates that there is a strong intermolecular π-π interaction. The Cu-Cu separation of 5.2038(11) Å is too far to have a magnetic exchange between the copper atoms.

Electronic spectra. The electronic spectrum of $[Cu(ppmma)Cl_2]_2$ in the nujol and methanol solution displays 702 and 741 nm, respectively. They are attributable to the d-d transition of the distorted square based pyramidal geometry around the Cu(II) ion, which is consistent with the literature report.[17] The electronic spectrum of the complex in methanol solution has a red shift (39 nm) when compared to the nujol electronic spectrum. This indicates that there is a deviation from the square based pyramidal environment of the complex when dissolved in methanol. The nujol electronic spectrum of $Cu(ppmma)Br_2$ exhibits an unique band at 514 nm and a broad band at 694 nm, which are assigned to d-d transitions of the copper(II) ion. This type of d-d spectrum is typical of a distorted square planar arrangement around the copper(II) ion which exhibits two bands near 530 and 630 nm.[18] The complexes $[Cu(ppmma)Cl_2]_2$ and $Cu(ppmma)Br_2$ exhibit a peak at 288 and 314 nm respectively, which are assigned to the intraligand transitions (π-π^*). A moderately intense peak at 376 nm for $[Cu(ppmma)-Cl_2]_2$ and 412 nm for $Cu(ppmma)Br_2$ are due to a ligand-to-metal charge transfer transition.

EPR spectral studies. The X-band EPR spectra of complex $[Cu(ppmma)Cl_2]_2$, both in the solid-state and frozen
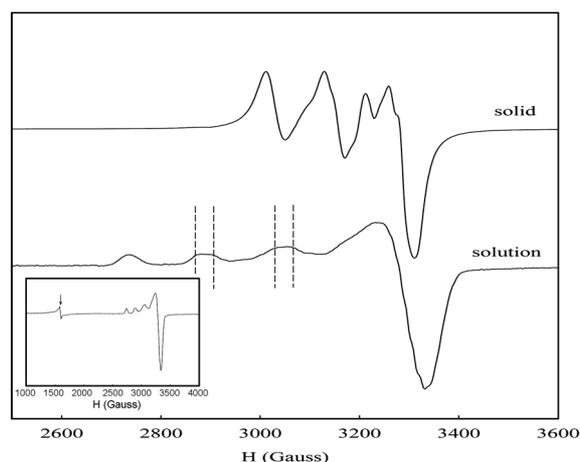
Figure 3. EPR spectra of $[Cu(ppmma)Cl_2]_2$ (powder & frozen glass solution spectrum in Toluene/MeOH); The insets show the sign at g ~ 4, around 1500 G in the range 1000-4000 G.

glass sample (Toluene/Methanol) at 77 K, are shown in Figure 3 and the corresponding data is summarized in Table 3. The solution EPR spectrum of $[Cu(ppmma)Cl_2]_2$ at 77 K shows a well-defined hyperfine structure in which the signal appears resolved with $g_\parallel$ (2.28) > $g_\perp$ (2.06) > 2.00, $A_\parallel$ = 151 G and $A_\perp$ = 32 G. The additional peak observed at 1500 G in the ESR spectrum (inset) yields a g value of 4.24, which is due to a singlet-triplet transition ($\Delta Ms = 2$), being coincident with a dimeric structure of the Cu(II) complex.[19] The EPR spectral features are a characteristic of typical axial symmetry with the unpaired electron in the d_{x2-y2} orbital. The hyperfine splitting signal of the parallel component of $[Cu(ppmma)Cl_2]_2$ in the solution is broadened when compared to the solid state. This observation is caused from the equilibrium between the mononuclear and binuclear complexes in the solution.[5,20] The solution and powder EPR spectrum of $Cu(ppmma)Br_2$ at 77 K exhibited an isotropic broad singlet with the value of $<g> \sim 2.0$.

Magnetic susceptibility measurements. The molar magnetic susceptibilities of the powder samples were measured with the temperature range 4-300 K. The χ_m and $1/\chi_m$ *vs.* T data of $[Cu(ppmma)Cl_2]_2$ are displayed in Figure 4. The χ_m value increases slowly as the temperature decreases and the χ_m values below 50 K show a sudden increase. The temperature variations of the magnetic susceptibility data of $[Cu(ppmma)Cl_2]_2$ and $Cu(ppmma)Br_2$ follow the Curie-Weiss law of the form $\chi = C/(T-\Theta)$. The Curie constant C = 0.45 and C = 0.44 K cm^3 mol^{-1} were obtained for $[Cu(ppmma)-Cl_2]_2$ and $Cu(ppmma)Br_2$, respectively. These values are

Table 3. UV-visible, EPR spectral and magnetic parameters for $[Cu(ppmma)Cl_2]_2$ and $Cu(ppmma)Br_2$ complexes

Complexes	UV-visible spectral data		EPR spectral data	Magnetic Properties	
	Nujol	Solution	Solution	θ(K)	C (Kcm^{3}mol^{-1})
$[Cu(ppmma)Cl_2]_2$	288, 376, 702	294, 741	$g_\parallel$ = 2.28; $g_\perp$ = 2.06; $A_\parallel$ = 151 G; $A_\perp$ = 32 G	1.64	0.45
$Cu(ppmma)Br_2$	314, 412, 514, 694	288, 350, 378, 754		−4.26	0.44
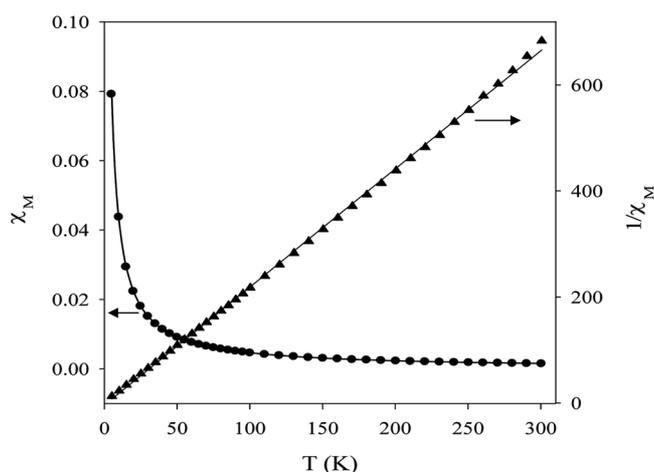
Figure 4. The plots of magnetic susceptibilities χ_m and $1/\chi_m$ *vs.* T in the temperature region of 4-300 K for [Cu(ppmma)Cl$_2$]$_2$. Calculated (—) and experimental (●) magnetic data are shown.

normal for a complex with one unpaired electron. The effective magnetic moment was calculated by the equation $\mu_{\text{eff}} = 2.828 \ [\chi \cdot T]^{1/2}$ and found to be 1.90 B.M. at room temperature for both compounds. These values are higher than spin-only value of 1.73 B.M.

Hatfield and co-workers[21] have shown that the singlet-triplet exchange coupling J varies in a regular way with the quotient θ/R, where θ is the Cu-Cl-Cu' bridging angle and R is the length of the super exchange pathway (R). It has been pointed out that for the values of the quotient between 32.6 and 34.8, the exchange interaction is ferromagnetic and the exchange interaction is antiferromagnetic for the values lower than 32.6 and higher than 34.8. In the case of our chloro-bridged dimer, [Cu(ppmma)Cl$_2$]$_2$, the value of the quotient θ/R is 33.29 Å^{-1}. It is observed that the J is nearly zero in this quotient value, suggesting that the super exchange coupling does not happen in [Cu(ppmma)Cl$_2$]$_2$, unlike our earlier reported[12] [Cu(dmamhp)Cl$_2$]$_2$ complex.

No significant magnetic interactions between the copper centers of dimer complexes which exhibit a square pyramidal geometry at the copper center of the mononuclear unit can be explained in terms of Hoffmann's theory.[22] The small J value of [Cu(ppmma)Cl$_2$]$_2$ complex is due to the near square pyramidal geometry ($\tau = 0.21$) of the copper center structure. An intramolecular interaction between the mononuclear units of [Cu(ppmma)Cl$_2$]$_2$ is not expected since the d$_{x2-y2}$ orbitals are positioned on the basal plane of each unit. The magnetic orbital of each copper, which is involved in the Cu-Cl-Cu bridge, is orthogonal to the d$_{x2-y2}$ orbital of the other copper ion also involved in the bridge.

Similar halide bridged dimeric copper complexes containing pyridine based ligand are currently under study, and the results will be reported along with the magneto-structural correlation.

Conclusion

We prepared the complex [Cu(ppmma)Cl$_2$]$_2$, which has a distorted square pyramid geometry with a nearly symmetric chloride bridge dimeric form. On the other hand, Cu(ppmma)-Br$_2$ has a distorted square planar geometry with a monomeric form. Both complexes exhibit strong π-π interactions and stabilize in solid state. The [Cu(ppmma)Cl$_2$]$_2$ complex remains paramagnetic with no magnetic interaction between the two copper ions although the fairly short Cu-Cu separation could lead to an interesting magnetic interaction between the metal ions at lower temperatures. This observation was explained in terms of a nearly square pyramidal geometry around the copper(II) center in the dimeric form. This work will be of much value in terms of complexes which find their application as a potential candidate for the magneto-structural correlation of halide bridged complexes.

References

1. Rodriguez-Fortea, A.; Alemany, P.; Alvarez, S.; Ruiz, E. *Inorg. Chem.* **2004**, *41*, 3769.
2. Rodriguez, M.; Llobet, A.; Corbella, M.; Martell, A. E.; Reibenspies, J. *Inorg. Chem.* **1999**, *38*, 2328.
3. Alves, W. A.; Almeida Santos, R. H.; Paduan-Filho, A.; Becerra, C. C.; Borin, A. C.; Costa Ferreira, A. M. *Inorg. Chim. Acta* **2004**, *357*, 2269.
4. Verdaguar, M. *Polyhedron* **2001**, *20*, 1115.
5. Youngme, S.; Cheansirisomboon, A.; Danvirutai, C.; Chaichit, N.; Pakawatchai, C.; Albada, G. A.; Reedijk, J. *Inorg. Chem. Commun.* **2006**, *9*, 973.
6. (a) Adhikary, C.; Mal, D.; Sen, R.; Bhattacharjee, A.; Gutlich, P.; Chaudhuri, S.; Koner, S. *Polyhedron* **2007**, *26*, 1658. (b) Hubert, S.; Mohamadou, A.; Gerard, C.; Marrot, J. *Inorg. Chim. Acta* **2007**, *360*, 1702.
7. Huang, W.; Hu, D.; Gou, S.; Qian, H.; Fun, H.-K.; Raj, S. S. S.; Meng, Q. *J. Mol. Struc.* **2003**, *649*, 269.
8. Braga, D.; Grepioni, F.; Desiraju, G. R. *Chem. Rev.* **1998**, *98*, 1375.
9. Burrows, A. D.; Chan, C.-W.; Chowdhry, M. M.; McGrady, J. E.; Mingos, D. M. P. *Chem. Soc. Rev.* **1995**, 329.
10. Liu, H. K.; Sun, W. Y.; Ma, D. J.; Yu, K. B.; Tang, W. X. *Chem. Commun.* **2000**, 591.
11. Fujita, M.; Yu, S.-Y.; Kusukawa, T.; Funaki, H.; Ogura, K.; Yamaguchi, K. *Angew. Chem. Int. Ed. Engl.* **1998**, *37*, 2082.
12. (a) Lee, Y.-M.; Lee, H.-W.; Kim, Y.-I. *Polyhedron* **2005**, *24*, 377. (b) Lee, H.-W.; Seo, H.-J.; Kim, H.-J.; Kang, S. K.; Heo, J. Y.; Kim, Y.-I. *Bull. Korean Chem. Soc.* **2007**, *28*, 885.
13. Kang, S. K.; Lee, Y.-M.; Kim, Y.-I.; Kim, Y.; Seff, K.; Choi, S.-N. *Inorg. Chim. Acta* **2004**, *357*, 2602.

14. Sheldrick, G. M. *Acta Cryst*. **2008**, *A64*, 112.
15. Addison, A. W.; Nageswara, R. T.; Reedijk, J.; Rijn, J.; Verschoor, G. *J. Chem. Soc. Dalton Trans.* **1984**, 1349.
16. Maroh, W. E.; Patel, K. C.; Hatfield, W. E.; Hodgson, D. *Inorg. Chem.* **1983**, *22*, 511.
17. Jadeja, R. N.; Shah, J. R.; Suresh, E.; Paul, P. *Polyhedron* **2004**, *23*, 2465.
18. (a) Gupta, N.; Gupta, R.; Chandra, S.; Bawa, S. S. *Spectrochim. Acta Part A* **2005**, *61*, 1175. (b) Lever, A. B. P. *Inorganic Electronic Spectroscopy*, 2nd ed.; Elsevier: Amsterdam, 1984.
19. (a) Estes, W. E.; Wasson, J. W.; Hall, W. E.; Hatfield, W. E. *Inorg. Chem.* **1978**, *17*, 3657. (b) Aggarwal, R. C.; Singh, N. K.; Singh, R. P. *Inorg. Chem.* **1981**, *20*, 2794. (c) Alves, W. A.; Almeida-Folho, S. A.; Santos, R. H. A.; Ferreira, A. M. D. C. *Inorg. Chem. Commun.* **2003**, *6*, 294.
20. Moncol, J.; Mudra, M.; Lonnecke, P.; Hewitt, M.; Valko, M.; Morris, H.; Svorec, J.; Melnik, M.; Mazur, M.; Koman, M. *Inorg. Chim. Acta* **2007**, *360*, 3213.
21. (a) Marsh, W. E.; Hatfield, W. E.; Hodgson, D. J. *Inorg. Chem.* **1982**, *21*, 2679. (b) Tosik, A.; Maniukiewicz, W.; Bukowska-Strzyzewska, M.; Mrozinski, J.; Sigalas, M. P.; Tipis, C. A. *Inorg. Chim. Acta* **1991**, *190*, 193. (c) Tuna, F.; Patron, L.; Journaux, Y.; Andruh, M.; Plass, W.; Trombee, J. *J. Chem. Soc. Dalton Trans.* **1999**, 539.
22. Hay, P. J.; Thibeault, J. C.; Hoffmann, R. *J. Am. Chem. Soc.* **1975**, *97*, 4884.